INTERNATIONAL CONFERENCE ON ELECTROMECHANICAL AND POWER SYSTEMS
October 4-6, 2007 - Chişinău, Rep.Moldova

TURBO-JET ENGINE'S ROTATION SPEED CONTROL SYSTEM WITH FUEL FLOW RATE INJECTION CONTROLLER

Alexandru Nicolae TUDOSIE

University of Craiova, Faculty of Electrical Engineering, Avionics Department,
E-mail: atudosie@elth.ucv.ro

***Abstract* – The paper presents a single-spool jet engine's rotation speed's control system, which has integrated a fuel flow rate injection controller meant to insure the speed and the temperature limitation during the engine's transient operating regimes. One has realized an improvement of the mathematical model for the system presented in [8] and, based on some experimental determination (for a VK-1F engine) and some graph-analytical estimation, one has elaborated a new non-linear model, respectively a linearized non-dimensional model. One has also performed a stability study and computer simulations, which determines the new domains' frontiers, comparing the system's operating with fuel injection controller and without it.**

***Keywords*:** *jet engine, rotation speed, control, fuel flow rate, controller, flight regime.*

1. INTRODUCTION

The integration of a fuel flow rate controller with an automatic rotation speed control system is meant to insure the limitation of the engine's speed and/or temperature increasing, to avoid the overshoots.
The paper deals with a single-spool jet engine, for the multi-spool engines the principles and the conclusions being similar.
Figure 1 presents a scheme of such an integrated system, based on a classic structure, using a fuel pump with mobile plate, a centrifuge rotation speed transducer and a hydraulic servo-amplifier with rigid feed-back [8], [6]. The fuel flow rate injection controller assists the hydraulic servo-amplifier, discharging its right active chamber during its operation [10].
System's main parts are: 1-single-spool turbo-jet engine; 2-fuel injection ramp; 3-turbo-compressor's shaft; 4-fuel pump; 5-fuel dosing element; 6-fuel tank; 7-centrifuge transducer; 8-centrifuge masses; 9-transducer's slide-valve; 10- feed-back's spring; 11-constant pressure valve; 12-rigid feed-back's slide valve; 13- feed-back's lever; 14-rotation speed's transducer's spring; 15-command lever (throttle connection); 16-glider; 17-STOP valve; 18-fuel injection pipe; 19-fuel pump's actuator's spring; 20-fuel pump's actuator's rod; 21- fuel pump's actuator; 22- fuel pump's actuator's piston; 23-pressure corrector; 24, 26-variable drossel; 25-sylphon; 27-controller's main spring; 28- fuel injection controller; 29-controller's elastic membrane; 30-pressure intakes; 31-controller's slide-valve.

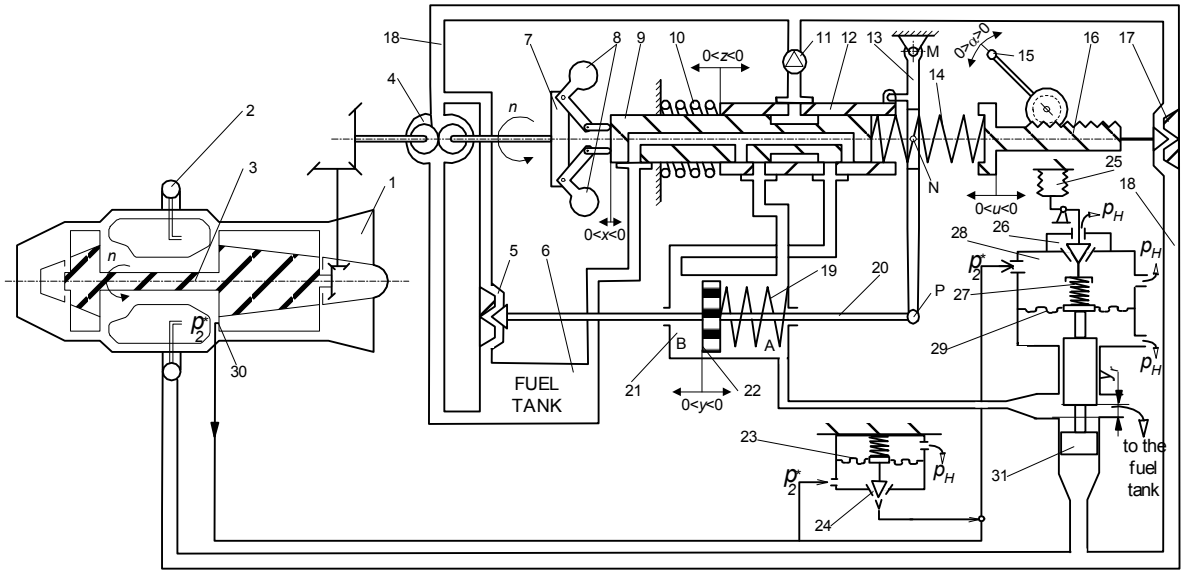

Figure 1.Integrated system's functional diagram

2. OPERATIONAL COUPLING BETWEEN THE SPEED'S CONTROLLER AND THE FUEL FLOW RATE CONTROLLER

The essential equations for the controller's identifying are [10] the slide-valve's (31) motion equation and the fuel flow rate's equation:

$$S_{31}p_i - S_m\left(p_m - p_1^*\right) = $$

$$= m_{31}\frac{\mathrm{d}^2 y_r}{\mathrm{d}t^2} + \xi\frac{\mathrm{d}y_r}{\mathrm{d}t} + k_{rm}y_r\,, \qquad (1)$$

$$\dot{M}_{cp} = \dot{M}_c\,, \qquad (2)$$

where S_{31} is the slide-valve's (31) frontal area surface, p_i -fuel's injection pressure (acting on the above mentioned area), p_m -active chamber's pressure, proportional to the compressor's exhaust pressure p_2^*, $p_m = p_m\left(p_2^*\right)$, p_1^* -compressor's intake pressure, y_r -slide valve's displacement, S_m - membrane's active area's surface, k_{rm} - spring (27)+membrane (29) connection's equivalent elastic constant, $\dot{M}_{cp}$ -pump's fuel flow rate, $\dot{M}_c$ -combustor injected fuel flow rate.

Assuming the same simplifying hypothesis [10], regarding the inertial effects, the fuel's compressibility, the viscous friction and the small p_1^* value, it results, for Eq. (1)

$$S_{31}p_i - S_m p_m = k_{rm}y_r\,. \qquad (3)$$

The fuel flow rate's expressions in (2) are, as presented in [8], [6] and [9]

$$\dot{M}_{cp} = k_{cp}ny\,, \qquad (4)$$

$$\dot{M}_c = k_{ci}\sqrt{p_i - p_{CA}} \approx k_{ci}\sqrt{p_i}\,, \qquad (5)$$

where y is the fuel pump's command part (plateau) displacement, n -fuel pump's and engine's rotation speed, p_{CA} -combustor's static pressure (which can be neglected versus the injection pressure p_i), k_{cp}, k_{ci} -amplifying co-efficient.

From Eq. (3) and (5) it results

$$S_{31}\left(\frac{\dot{M}_c}{k_{ci}}\right)^2 = S_m p_m(p_2^*) + k_{rm}y_r \qquad (6)$$

and, considering the fuel pump's actuator's simplified equation [6] as

$$\left(T_{sp}'\mathrm{s}+1\right)y = k_m y_r\,, \qquad (7)$$

Eq. (2) and Eq. (4), it results

$$\left(T_{sp}'\mathrm{s}+1\right)\dot{M}_c = n\frac{k_{cp}k_m}{k_{rm}}\left[S_{31}\left(\frac{\dot{M}_c}{k_{ci}}\right)^2 - S_m p_m(p_2^*)\right], \qquad (8)$$

which, considering also Eq. (2), leads to

$$\mathrm{s}\dot{M}_c = \frac{1}{T_{sp}'}\left\{n\frac{k_{cp}k_m}{k_{rm}}\left[S_{31}\left(\frac{\dot{M}_c}{k_{ci}}\right)^2 - S_m p_m(p_2^*)\right] - \right.$$

$$\left. - \dot{M}_{cp}\right\} = \frac{\mathrm{d}\dot{M}_c}{\mathrm{d}t}\,. \qquad (9)$$

So, one can observe that $\frac{\mathrm{d}\dot{M}_c}{\mathrm{d}t} = f(n, \dot{M}_c, p_2^*)$, that means that fuel flow rate's variation's velocity is a function of the engine's rotation speed, compressor's exhaust pressure, but of the flow rate itself too.

From Eq. (9), as well as from the observation that the compressor's exhaust pressure is a function of $\dot{M}_c$ too, it results

$$\frac{\mathrm{d}\dot{M}_c}{\mathrm{d}n} = \frac{\pi J}{30}\frac{f(n, \dot{M}_c, p_2^*)}{M_{GTC}\left(n, \dot{M}_c\right)}, \qquad (10)$$

so a non-linear function of two variables *n* and $\dot{M}_c$.

Figure 2 presents a graph-analytical relation between these two parameters, but under a non-dimensional form, that means that $\frac{\dot{M}_c}{\left(\dot{M}_c\right)_{\max}} = f\left(\frac{n}{n_{\max}}\right)$, for an old VK-1F engine [11].

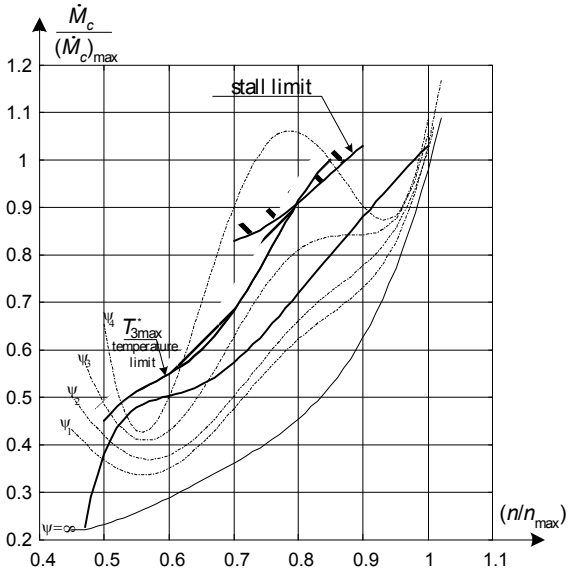

Figure 2. Fuel flow rate versus rotation speed characteristic for a turbo-jet engine (VK-1F)

3. INTEGRATED SYSTEM'S MATHEMATICAL MODEL

The effects of the integrated controller's operating could be revealed by the engine's speed control system's mathematical model's modifications, which model was presented in [8].

Assuming that the compressor's pressure ratio $\pi_c^* = \frac{p_2^*}{p_1^*}$ is a function of its rotation speed, one can express the exhaust pressure's relative parameter as

$$\overline{p_2^*} = \overline{p_1^*} + k_{np2}\overline{n}, \tag{11}$$

where the co-efficient $k_{np2} = \frac{n_0}{\pi_{c0}}\left(\frac{\partial \pi_c^*}{\partial n}\right)_0$. The controller's block diagram with transfer functions, presented in [9], can be represented in an equivalent form, which lays in figure 3.

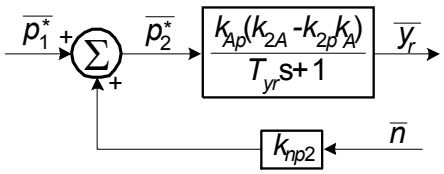

Figure 3. Fuel flow rate's controller's equivalent block diagram with transfer functions

The connection (17) is discharged by the controller's slide-valve, so the fu3el flow rate through this one is

$$Q_r = \mu_r b_r \left(y_r - y_{rs}\right)\sqrt{\frac{2}{\rho}}\sqrt{p_A - p_{sc}}\,, \tag{12}$$

where μ_r-flow rate co-efficient of the connector (17), b_r-connector's width, y_{rs}-steady state value of the slide=valve displacement, p_A-fuel pressure in actuator's active chamber A, p_{sc}-low pressure circuit's pressure value (neglected versus p_A).

One assumes that a generic variable X has the form $X = X_0 + \Delta X$, so, expressing like this each variable, the equation (12) becomes

$$\Delta Q_r = K_{rs}\Delta y_r + K_{prA}\Delta p_A, \tag{13}$$

where $K_{sr} = \left(\frac{\partial Q_r}{\partial y_r}\right)_0 = \mu_{r0} b_r \sqrt{\frac{2}{\rho}}\sqrt{p_{A0}}$,

$$K_{prA} = \left(\frac{\partial Q_r}{\partial p_A}\right)_0 = -\frac{1}{2}\mu_{r0} b_r y_{r0}\sqrt{\frac{2}{\rho}}\frac{1}{\sqrt{p_{A0}}}. \tag{14}$$

The total fuel flow rate eliminated of the A chamber is $Q_A + Q_r$, so the mathematical model's equations in [8] will be modified, based on the same assumptions, as follows

$$\Delta Q_A + \Delta Q_r = K_{sx}\Delta x - K_{sz}\Delta z + K_{rs}\Delta y_r - \left(K_p - K_{prA}\right)\Delta p_A, \tag{15}$$

$$\Delta Q_A + \Delta Q_r = \beta V_{A0}\frac{\mathrm{d}}{\mathrm{d}t}\Delta p_A + S\frac{\mathrm{d}}{\mathrm{d}t}\Delta y + K_{sr}\Delta y_r + K_{prA}\Delta p_A. \tag{16}$$

Similarly, one can express the equations for the flow rate and the pressure in chamber B; adding those two equations, it results

$$K_{sx}\Delta x - S\frac{\mathrm{d}}{\mathrm{d}t}\Delta y - K_{sz}\Delta z + K_{sr}\Delta y_r = \frac{\beta V_0}{2}\frac{\mathrm{d}}{\mathrm{d}t}\left(\Delta p_A - \Delta p_B\right) + \frac{K_p}{2}\left(1 - \frac{K_{prA}}{K_p}\right)\left(\Delta p_A - \Delta p_B\right) \tag{17}$$

The non-dimensional form of the above equation is, after the Laplace transformation,

$$k_{sx}\bar{x} - k_{sz}\bar{z} + k_{sr}\bar{y}_r - k_{sy}\mathrm{s}\bar{y} = \frac{1}{k_{Ap}^{/}}\left(T_{sp}^{/}\mathrm{s}+1\right)\left(\bar{p}_A - \bar{p}_B\right), \tag{18}$$

where $k_{Ap}^{/} = \frac{2}{K_p - K_{prA}} = \frac{k_{ap}}{1 - \frac{K_{prA}}{K_p}}$, $k_{sr} = \frac{2K_{sr}y_{r0}}{p_a}$,

$$T_{sp}^{/} = \frac{\beta V_{A0}}{K_p - K_{prA}} = \frac{T_{sp}}{1 - \frac{K_{prA}}{K_p}}. \tag{19}$$

The new form of the integrated system's mathematical model becomes ([8], [9], [10])

$$\left(T_M\mathrm{s}+1\right)\bar{n} = k_c\dot{\overline{M}}_c - k_{p1}\overline{p_1^*}, \tag{20}$$

$$\overline{M}_c = k_{pn}\bar{n} + k_{py}\bar{y}, \tag{21}$$

$$\bar{x} = k_u\bar{u} - k_{es}\bar{n}, \tag{22}$$

$$\bar{u} = k_{u\alpha}\bar{\alpha}, \tag{23}$$

$$k_{sx}\bar{x} - k_{sz}\bar{z} + k_{sr}\bar{y}_r - k_{sy}\mathrm{s}\bar{y} = \frac{1}{k_{Ap}^{/}}\left(T_{sp}^{/}\mathrm{s}+1\right)\left(\bar{p}_A - \bar{p}_B\right), \tag{24}$$

$$\bar{y} = k_{yp}\left(\bar{p}_A - \bar{p}_B\right), \tag{25}$$

$$\bar{z} = r_l\frac{y_0}{z_0}\bar{y}, \tag{26}$$

$$k_i\bar{p}_i - k_{rp2}\overline{p_2^*} + k_{rp1}\overline{p_1^*} = \left(T_{yr}\mathrm{s}+1\right)\bar{y}_r, \tag{27}$$

$$\overline{p_2^*} = \overline{p_1^*} + k_{np2}\bar{n}. \tag{28}$$

Based on the above determined non-dimensional linear mathematical model, one has determined the block diagram with transfer functions, presented in figure 4.

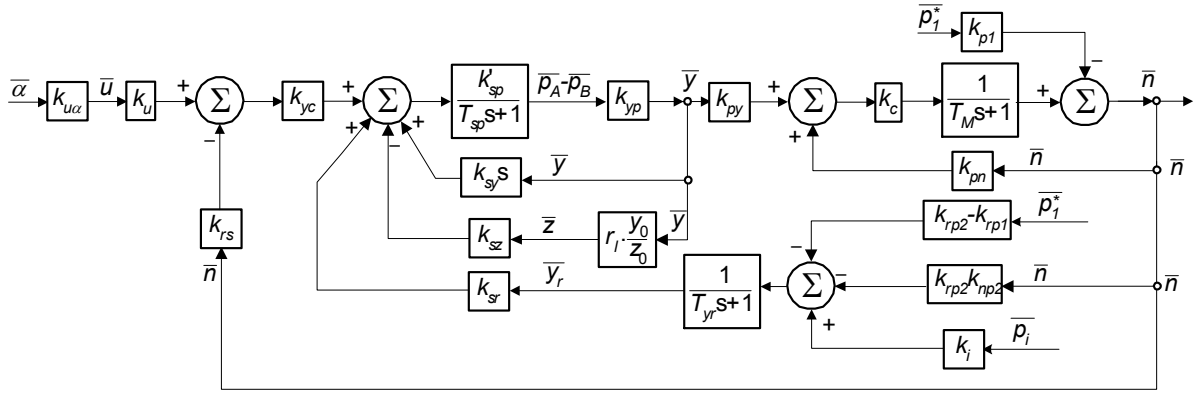

Figure 4. Integrated system's block diagram with transfer functions

4. INTEGRATED SYSTEM'S STABILITY AND QUALITY

4.1. About actuator's constants

One can observe that both of the actuator's constants are modified with respect to their initial forms [8]:

$$T_{sp} = \frac{\beta V_{A0}}{K_p},\ k_{ap} = \frac{2}{K_p}, \tag{29}$$

being bigger then these ones, because of $K_{prA} < K_p$. Obviously, the situation $K_{prA} \geq K_p$ is senseless, because in this case the constants T'_{sp} and k'_{ap} are becoming negatives, tending to $-\infty$! So, the condition for T'_{sp} and k'_{ap} existence is

$$\left(\frac{\partial Q_A}{\partial p_A}\right)_0 > \left(\frac{\partial Q_r}{\partial p_A}\right)_0, \tag{30}$$

equivalent to

$$y_{r0} > \frac{b}{b_r}(x_0 - z_0), \tag{31}$$

which leads to the condition for the maximum slide-valve's stroke $(y_r)_{\max}$

$$(y_r)_{\max} > \frac{b}{b_r}(x_{\max} - z_{\max}) = \frac{b}{b_r}(x_{\max} - r_l y_{\max}). \tag{32}$$

The growth of the co-efficient K_{prA}, obviously, inside the above determined limits, involves the growth of the T'_{sp} and k'_{ap} values (see figure 5), theoretically to ∞, extreme value obtained hypothetically when K_{prA} becomes equal to K_p, situation which corresponds to the permanent actuator's active chamber's discharging, equivalent to the actuator's inactivation.

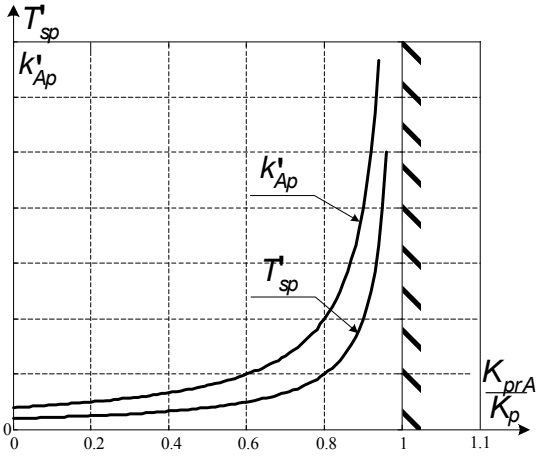

Figure 5. Actuator's time constant and amplifying constant versus the co-efficient ratio $\frac{K_{prA}}{K_p}$

4.2. System's stability

Considering the actuator's new transfer function as having the form $H'(s) = \frac{1}{\tau'_s s + \rho_s}$, one can observe that the stability constant ρ_s has the same expression as in [8], similar to the one in [6],

$$\rho_s = \frac{y_0}{x_0}\frac{S}{\mu b}\sqrt{\frac{\rho}{p_a}}, \tag{33}$$

but the new time constant τ'_s behave itself just like T'_{sp}, becoming bigger then τ_s if the condition (30) is fulfilled

$$\tau'_s = \frac{\tau_s}{1 - \frac{K_{prA}}{K_p}} > \tau_s. \tag{34}$$

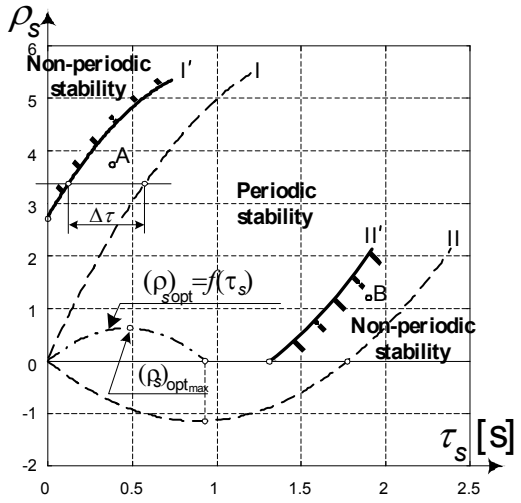

Figure 6. Actuator's stability domains

In a (ρ_s, τ_s) frame, as the one in figure 6, built as it is shown in [6] and [8], the point representing the assisted actuator is horizontally displaced to the right, being possible to change its stability domain. So, rapid actuators, which have great stability constants ρ_s values and small time constants values, pass from the non-periodical stability to the periodical stability (see point A in fig. 6); in the mean time, slow actuators, which have small stability constants ρ_s values and great time constants values, pass from the periodical stability to the non-periodical stability (see point B in fig. 6).

The situation B represents the favorable situation, when the controller improves the actuator's (and the control system's) behavior; in opposite, situation A represents the unfortunate situation, when the actuator's (and the control system's) behavior gets worse because of the controller using. One can observe that the controller using is equivalent to a displacement to the left of the stability limits (curves I and II), displacement equal to

$$\Delta\tau = \tau_s^{/} - \tau_s = \frac{\frac{K_{prA}}{K_p}}{1-\frac{K_{prA}}{K_p}}\tau_s , \qquad (35)$$

until them reach the new positions $I^{/}$ and $II^{/}$. So, in order to assure an appropriate operating of the integrated system, one must choose the appropriate and convenient combination between the actuator's constants, even in the pre-design stage.

4.3. System's quality

The controller's operating modifies the whole system's quality. One has performed some simulations, using VK-1 engine's experimental and analytic data.

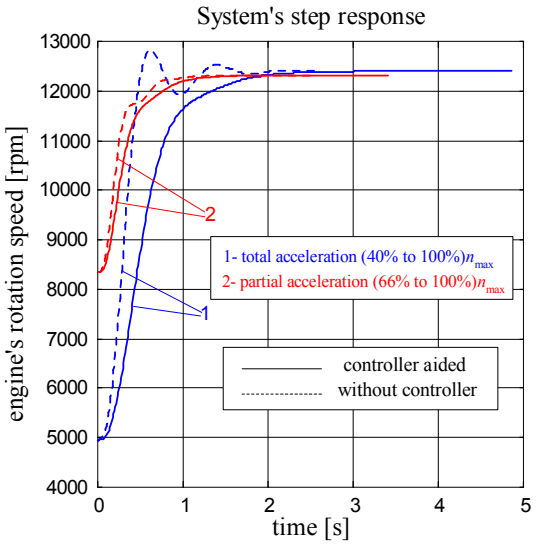

Figure 7. Aided and non-aided system's step response, from the engine's rotation speed's point of view, for a constant flight regime (H=0 m, V=0 km/h)

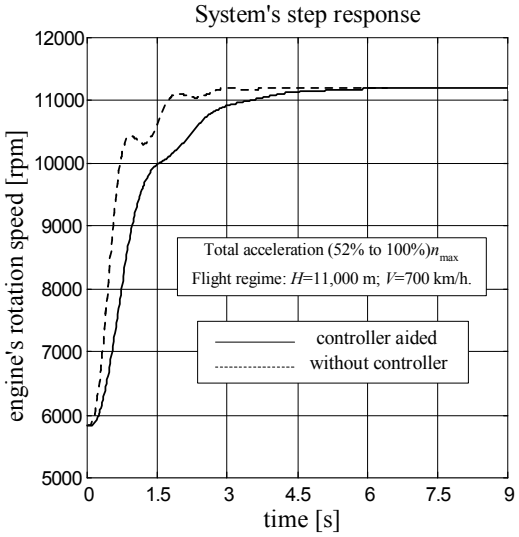

Figure 8. Aided and non-aided system's step response from the engine's rotation speed's point of view, for an intense constant flight regime

Some of the simulation's result, concerning the controller aided and non-aided system's step response, are shown in figures 7 to 9. The step input for the engine corresponds to a throttle "step handle" (throttle's instant displacement from its current position to its extreme position - maximum or minimum).

Figure 7 shows the engine's behavior (time response) for a constant flight regime ("at the ground" H=0, V=0), for step input, in two cases: 1-for a complete acceleration, 2-for a partial acceleration; system's response is presented in both situations: without controller (dash-line) and controller aided (continuous line). One can observe that the engine is, in any case, a stabile system from the rotation speed's

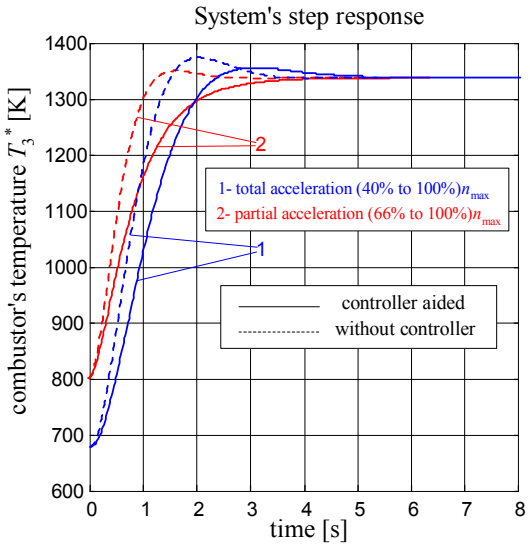

Figure 9. Aided and non-aided system's step response, from the engine's combustor's temperature's point of view, for a constant flight regime (H=0 m, V=0 km/h)

n point of view, but the non-aided system could have a periodical behavior, especially for the total acceleration. If the flight regime changes (flight altitude and speed are growing), the non-aided system becomes periodical stabile, which is not an appropriate behavior, but if the controller becomes active, the stability tends to regain its non-periodical character (see figure 8).

Figure 9 shows the engine's behavior in the same situations and flight regime from the combustor's temperature T_3^* point of view.

5. CONCLUSIONS

Starting from earlier studied automatic control systems for turbo-jet engines, one has performed some studies concerning mathematical models and simulations for integrated control systems, particularly for a rotation speed control system based on the fuel flow rate control and a specific fuel rate controller for dynamic (transient) regimes.

For the studied case, one can make some important observations:

- the integrated system (connection between the turbo-jet engine, the fuel pump and its regulator and the fuel flow rate controller) is a stabile system in any studied case;
- system's stability is both periodical and non-periodical, but the controller's using tends to transform the periodical stability into a non-periodical one;
- engine's time responses are bigger for the controller aided one, so the engine becomes "slower" but safer, because of the overshoots due to the periodic behavior eliminating/diminishing, both for the rotation speed and (more important) for the combustor's temperature. One can affirm that, in most of cases, the fuel flow rate controller has eliminated the over-speeding and the over-heating, or brought them into acceptable limits, which makes the engine more reliable, extends its life and service duration and reduces its maintenance/overhaul costs;
- the flight regime's intensity's growing makes the aided engine's time response until 80% bigger than the non-aided one's, but the advantages are the same, the periodic behavior being eliminated or diminished.

References

[1] Abraham, R. H. *Complex dynamical systems.* Aerial Press, Santa Cruz, California, 1986.

[2] Dodescu, Gh., a. o. *System's simulation.* Military Publishing, Bucharest, 1986.

[3] Goewski, S. A. *Aircraft Gas Turbine Propulsion Systems' Automation* U.S.S.R, Military Publishing, Moscow, 1980.

[4] Lungu, R. Tudosie, A. *Studies concerning some follower systems.* Proceedings of the International Conference SIELMEC 2001, Chisinau, Rep. Moldova, 4-5 october 2001, pp. 74-81.

[5] Manole, I. *Design solutions for Aircraft Turbo-jet Engines*, vol. I, II; Technical Military Academy in Bucharest Publisher, 1978.

[6] Stoenciu, D. *Aircraft Engines' Automation. Turbo-jet Engines' Rotation Speed Automatic Control.* Technical Military Academy in Bucharest Publisher, 1976.

[7] Stoicescu, M., Rotaru, C. *Turbo-Jet Engines. Characteristics and control Methods* Technical Military Academy in Bucharest Publisher, 1999.

[8] Tudosie, A. *Hydro-mechanical Automatic Control System for a Turbo-jet Engine.* Proceedings of the Conference "25 Years of Technical High Education", Arad, Romania, 30-31st october 1997, section 8 pp. 177-184.

[9] Tudosie, A. *Fuel Flow Rate Automatic Controller with Barostatic Corrector.* Proceedings of the Thermotechics National Conference, Naval Academy "Mircea cel Batrin" Anniversary Session, Constanta, Romania, 14-15th november 2002, vol II, pp. 253-263.

[10] Tudosie, A. *Fuel Flow Rate Controller With Respect to the Compressor's Pressure Ratio.* Proceedings of the International Conference SIELMEN 2007, Chisinau, Rep. Moldova, 4-6 october 2007.

[11] *** *VK-1A, VK-1F Engines - Overhaul and Maintenance Manual.*